Minireview

Computational studies of proton transport through the M2 channel

Yujie Wu, Gregory A. Voth*

Department of Chemistry and Henry Eyring Center for Theoretical Chemistry, University of Utah, 315 S. 1400 E. Rm. 2020, Salt Lake City, UT 84112-0850, USA

Received 18 March 2003; accepted 5 June 2003

First published online 17 July 2003

Edited by Maurice Montal, Gerhard Thiel and Anna Moroni

Abstract The M2 ion channel is an essential component of the influenza A virus. This low-pH gated channel has a high selectivity for protons. Evidence from various experimental data has indicated that the essential structure responsible for the channel is a parallel homo-tetrameric α-helix bundle having a left-handed twist with each helix tilted with respect to the membrane normal. A backbone structure has been determined by solid state nuclear magnetic resonance (NMR). Though detailed structures for the side chains are not available yet, evidence has indicated that His37 and Trp41 in the α-helix are implicated in the local molecular structure responsible for the selectivity and channel gate. More definitive conformations for the two residues were recently suggested based on the known backbone structure and recently obtained NMR data. While two competitive proton-conductance mechanisms have been proposed, the actual proton-conductance mechanism remains an unsolved problem. Computer simulations of an excess proton in the channel and computational studies of the His37/Trp41 conformations have provided insights into these structural and mechanism issues.

Key words: Influenza A virus M2 ion channel; Gating mechanism; Selectivity mechanism; Proton transport

1. Introduction

The influenza A virus M2 ion channel is a proton-selective channel formed by the transmembrane (TM) domain of the M2 protein – an integral membrane protein of the influenza A virus [1–4]. When the environmental pH (pH_{out}, pH at the extracellular side of the M2 channel) goes lower than a threshold (for example, pH 6), the channel is activated and selectively transports protons across the membrane from its N-terminal/extracellular side to its C-terminal/cytoplasmic side [2,5], thus providing a controlled pH-regulating mechanism for the vesicular compartment with the M2 protein embedded in the membrane.

The M2 channel has been found crucial in the viral life cycle. During the viral uncoating process, when the virion is internalized into the endosome, the M2 protein can acidify the virion interior, promoting the dissociation of the viral matrix protein (M1) from the ribonucleoprotein (RNP), which is a crucial step for the transport of the RNP from the virion into the cell's nucleus [6–9]. For some influenza virus subtypes, it was found that the M2 channel can elevate the intravesicular pH of the trans-Golgi network, preventing the viral protein haemagglutinin, which is transported to the cell surface through the trans-Golgi network, from incorrect maturation in an otherwise low pH environment [10–13]. Blocking the M2 channel by the anti-flu drug amantadine (1-aminoadamantine hydrochloride, AMT) has been shown to interrupt both parts of the viral life cycle [8,10–12].

Due to these essential roles of the M2 channel in the viral life cycle, study of its structure and functions at various levels of molecular detail is of great interest to anti-flu drug design, pharmacology and medicine.

2. The architecture of the M2 channel

The gene for the M2 peptide has been cloned and sequenced [14–16], revealing a 97-amino-acid primary structure, which can fold into three structural domains: a 24-residue N-terminal/extracellular domain, a 19-residue TM domain, and a 54-residue C-terminal/cytoplasmic domain [17]. A considerable amount of experimental evidence has indicated that the M2 protein is a parallel homotetramer of the M2 peptide [1,18–24], and the subunits are held together mainly by non-covalent interactions and further stabilized by inter-subunit disulfide links in the N-terminal domain [1,18,21,25]. The TM domain is the main channel-formation structure and is directly responsible for multiple molecular functions, for example, the selective filter, the channel gate, and the interaction sites of the AMT inhibitor. The 19 residues in the TM domain are mostly hydrophobic, with the exceptions of Ser31, Gly34, His37, and they can form one α-helix strand spanning the hydrocarbon region of the membrane; the tetramer architecture enables an aqueous pore to be lined by the TM domains across the membrane. The amino acid residues in the pore-facing side of the putative α-helix were deduced from mutagenesis [3]. They are Val27, Ala30, Ser31, Gly34, His37, Leu38 and Trp41. Their mutations were also shown to affect

*Corresponding author. Fax: (1)-801-581 4353.
E-mail address: voth@chem.utah.edu (G.A. Voth).

Abbreviations: pH_{out}, pH at the extracellular side of the M2 channel; TM, transmembrane; RNP, ribonucleoprotein; AMT, 1-aminoadamantine hydrochloride; M2-TMP, M2 transmembrane peptide; SDS, sodium dodecyl sulfate; DMPC, dimyristoylphosphatidylcholine; MD, molecular dynamics; MS-EVB, multistate empirical-valence bond; UVRR, UV resonance Raman

0014-5793/03/$22.00
doi:10.1016/S0014-5793(03)00779-8

both the channel activity and AMT sensitivity. The putative α-helix secondary structure for the TM domain received further support by a Fourier analysis on a Cys scanning mutagenesis result, which revealed a periodicity consistent with the α-helix structure and also suggested that the overall structure of the TM domain is a left-handed coiled-coil or a helix bundle [20].

A synthetic 25-residue peptide (M2-TMP) with the amino acid sequence as follows: NH2-Ser-Ser-Asp-Pro-Leu-Val-Val-Ala-Ala-Ser-Ile-Ile-Gly-Ile-Leu-His_{37}-Leu-Ile-Leu-Trp_{41}-Ile-Leu-Asp-Arg-Leu-COOH, which corresponds to the residues 22–46 (encompassing the segment for the TM domain, residues 25–43) in the M2 protein, has been found to be able to form an AMT-sensitive proton-selective channel in lipid bilayers with similar specificity and efficiency to the whole M2 protein [23,26]. It was shown to form tetramers in lipid micelles [21,23]. Circular dichroism data indicated that the secondary structure of the peptide is predominantly α-helix, which is not affected by temperature and AMT [27]. The helix tilt angle with respect to the membrane normal and the rotational angle around the helix axis were determined by both site-directed infrared dichroism spectra [28] and solid state nuclear magnetic resonance (NMR) [29–32]. These results suggested a range of 30–40° for the tilt angle and roughly −50° for the rotational angle. The latter also confirmed the peptides are almost ideal α-helices that are not affected by the presence of AMT. The determined tilt angles support that the M2-TMP channel should be left-handed so that the hydrophilic residues can be oriented towards the pore lumen [33]. Recently, the tilt angle for the TM domain of the whole M2 protein in liposomes was also determined, revealing a smaller value of 25° ± 3 [24]. The reason for the reduced tilt angle has not been fully understood; it could be due to the greater intersubunit interactions in the whole protein or just the different experimental conditions.

3. Two ion-conductance mechanisms

The proton selectivity and channel gating are the key biological functions of the M2 channel. The channel is highly proton-selective – at least 10^6-fold more conductive than other cations [34,35]. The channel is low-pH gated, undergoing a 50-fold conductance increase from pH 8.2 to pH 4.5 [35,36]. The detailed structure responsible for these functions remains unclear.

Several lines of evidence have suggested that a highly conservative residue His37, which is the only ionizable residue in the TM domain around pH 6, plays a crucial role. Especially strong evidence was gained from mutagenesis studies, which show that mutating this residue can greatly alter the conductance behavior. For example, replacing it with Ala, Glu or Gly results in a large increase in proton conductance and loss of pH-induced gating behavior though the current–voltage relationship and amantadine sensitivity are preserved [2,36]. Replacing it with Glu also results in reduced selectivity [36], while mutating it to Cys completely abolishes its channel function [37]. Data on the Cu^{2+} inhibition of the M2 channel [38] and on pH titration [36] also suggests that the His37 is implicated in the selective filter.

Extensive molecular modeling studies have contributed to the elucidation of the structure–function relationship of the M2 channel [20,39–45]. For the closed state, most proposed models orient the four His37's in such a way that their imidazole side chains are directed toward the lumen, thereby occluding the pore and forming a channel gate. For the open state, however, the models diverge, resulting in two possible conductance mechanisms, namely the gating mechanism and the shuttle mechanism.

In the gating mechanism [39], when the channel is activated, each of the histidines' imidazole moieties can acquire an additional proton and become positively charged. The protons are not immediately released back to the pore water; instead, the histidine residues bind them (at least for a relatively long time). Then, due to the electrostatic repulsion between the positive charges, the imidazole side chains sway away from each other, thus opening the otherwise occluded pore to let the pore water penetrate through to form a continuous proton-conductive water wire (proton wire).

In contrast to the gating mechanism, the histidine residues in the proposed shuttle mechanism are directly involved in a proton relay [20]. In this mechanism, when the channel is activated, an imidazole side chain accepts the excess proton to form a bi-protonated intermediate, which is presumed to be short-lived and tends to release either the ε- or δ-hydrogen back to the pore water to become neutral again (proton shuttling). Transport of a single proton through the gate is accomplished when the hydrogen at the opposite side is released to the pore water. Then to transport the next proton, the initial state needs to be regenerated, which was hypothesized to occur through tautomerization or just flipping of the imidazole ring. Efficient transport through the gate requires the orientation of the imidazole rings to allow the $N_\varepsilon - N_\delta$ vector, i.e. the one formed by the N_ε and N_δ atoms of the same imidazole group, to be nearly parallel to the channel axis so that the two nitrogen atoms can form hydrogen bonds with pore waters. This conformation requires that the δ-nitrogen is pointed to the channel's N-end (otherwise the vector cannot be parallel), so to be able to accept an additional proton the histidine must not have δ-hydrogen in its mono-protonation state.

Recently, a UV resonance Raman (UVRR) spectroscopy study reported the detection of bi-protonated histidine in the activated state of the M2-TMP channel [46], supporting the gating mechanism. The study also suggested that the histidine residues are probably fully bi-protonated since the addition of sodium dodecyl sulfate (SDS), which was expected to disrupt the bundle structure and expose the subunits to the solution, did not yield an increase of the corresponding Raman intensity for the bi-deuterated imidazole moieties. However, due to that no evidence was provided to show the subunits were exposed to the solution upon addition of SDS, the exact number of bi-protonated histidine residues in the open state remains a problem to be clarified in the future.

4. Molecular dynamics (MD) simulation of proton transport in the M2 channel

The two conductance mechanisms have also been studied through classical MD simulations of an M2-TMP model embedded in a fully solvated dimyristoylphosphatidylcholine (DMPC) bilayer [45]. Through analyzing the structural stability of the channel and the pore water structure, it was found that within the time scale the simulations reached (roughly 1 ns), a fully bi-protonated state destabilizes the channel structure while a doubly bi-protonated state leads to a deformed,

Fig. 1. Stereo representation of the averaged backbone structure from simulation (red) superimposed on the NMR backbone structure (green). The backbones are represented in tube mode.

yet closed, structure, thus making the shuttle mechanism more favorable.

An explicit simulation of the excess proton in the M2 channel was recently accomplished in our group [44] with the aid of a multistate empirical-valence bond (MS-EVB) model for proton transport in aqueous systems [47–53]. Though this work did not focus on the detailed side chain structure, it presented a different view on the conductance mechanism in terms of the proton transport. The simulations were carried out on the TM domain in a fully solvated DMPC bilayer with a presumption that one stable bi-protonated His37 might somewhat open the channel for protons. Seven MD simulation trajectories were obtained with different starting configurations, in all of which the excess proton was placed inside the channel at different positions near the N-end and the M2 channel has one His^+ and three neutral His's, which can neither accept nor donate a proton. Indeed, within the time scales reached by the trajectories (500–1000 ps), the proton was observed to pass through the channel at different times in three of the seven trajectories. Although the applied TM electric field (100–200 mV) may complicate these conclusions, this result lends direct support to the gating mechanism. However, as opposed to the picture of the gating mechanism described previously, our MD study suggests that one (or maybe two) bi-protonated histidine may be sufficient for opening the channel for protons while still keeping it closed for other ions. Moreover, the presence of one positive charge near the constrictive region formed by the His37 residues seems not to lead to a barrier too high for protons to pass through.

Our MD study presents a very detailed picture of the explicit proton transport in the M2 channel for the first time. For example, it was confirmed that as in bulk water the excess proton in the channel is transferred via the so-called *structural diffusion* mechanism, where the excess proton's solvation structure rather than the hydronium ion is propagated in space [54,55]. It was also found that the excess proton favors an Eigen-like solvation structure in the channel similar to that in the bulk water; however its overall diffusion constant may be reduced by the channel by up to a factor of three or it may even be immobilized in some situations for long periods of time. It also illustrated the importance of the protein dynamics for proton's motion in the channel – a frozen channel can effectively immobilize the otherwise transferring excess proton. Further MS-EVB simulations addressing the conductance mechanism including explicit ionizable histidine groups and a more detailed examination of the protein's conformational and dynamical effects on proton transport are currently underway in our group.

5. Possible closed and open conformations and their implication for the proton-conductance mechanism

We have recently compared the M2 channel model used in our previous work with the available NMR backbone structure. The averaged tilt angles for each helix in our MD simulations are 47°, 42°, 39°, 38° with standard errors around 5, putting them in good agreement with the experimental value (30–40°) [28–32]. The averaged rotational angles for each helix are 12°, 1°, −22°, −20°, deviating substantially from the reported experimental value (−62–−43°). However, this model

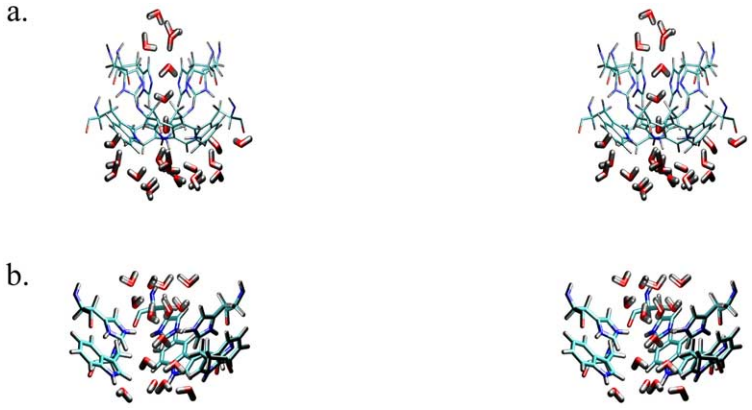

Fig. 2. Stereo representations of simulation snapshots of the closed (a) and open (b) structures of His37, Trp41, and nearby pore water molecules. The closed structure is a typical (t60, t90, δ) conformation of the His37 and Trp41 residues. Note that the water molecules near the histidine have opposite orientations, which interrupts the 'proton wire'. The proposed open channel structure is obtained by rotating the χ_2 angle of each His37 from 60° to 0°, while the structure of Trp41 maintains a typical t90 conformation. Note that the pore water molecules can penetrate through the constrictive gate region near His37. One pair of His37 and Trp41 is omitted in the open structure for the sake of clarity.

is perhaps the best case achieved today for the M2 system using computer modeling without previous knowledge of experimental structural data. Fig. 1 is a superimposed picture of the averaged backbone structure from the simulation on the NMR structure, showing their closeness in the overall structure. Some comparisons between other models and the NMR structure may be found in the literature [29].

Several recent experimental studies have suggested the involvement of the Trp41 residues in channel gating. For example, a UVRR spectroscopy study has suggested that Trp41 may have cation–π interaction with the bi-protonated histidine residue in the open state [46]. The role of Trp41 for the closed state was also investigated via mutagenesis and electrophysiological experiments, which indicated that mutating Trp41 to Phe, Cys or Ala results in 'leaky' channels, which can transport protons outward (i.e. from the C-end to the N-end), thus Trp41 was proposed to be the actual channel gate [56]. Cross and coworkers recently determined that the distance between the N_δ-His37 and C_γ-Trp41 should be less than 3.9 Å for the closed channel [57], further implying the involvement of Trp41 in channel gate. Based on this information and the previously determined NMR backbone structure, they proposed a closed structure with the (t-160, t-105) conformation for His37 and Trp41. [The notation – (t-160, t-105) – means that the conformations of His37 and Trp41 are the t-160 and t-105 rotamers, respectively. The nomenclature for rotamers here follows the Penultimate Rotamer Library [58]. When the mono-protonation state of the histidine is taken into account, the symbol δ or ε is added – for example, (t-160, t-105, δ) – to indicate the histidine is δ- or ε-monoprotonated, respectively].

Based on the same structural information [57], however, an alternative conformation for His37 and Trp41 – (t60, t90, δ) – for the closed state of the M2 channel has been proposed by our group (to be published). This result was obtained via a thorough scan over the conformational space followed by energetic (ab initio) and functional assessment. A representative structure of this conformation shows that a constrictive region is formed by both His37 and Trp41 (Fig. 2a) and the δ-hydrogen of His37 is pointed toward the indole ring of Trp41, implying a hydrogen–π interaction that can stabilize each other's conformation. This model seems consistent with almost all observed phenomena about His37 and Trp41 in experiments that we know. For example, the pore waters near His37 have an opposite orientation, explaining why the channel does not conduct protons if the histidine residues are neutral. The conformation of Trp41 prevents His37 from being exposed to the bulk water at the C-end, suggesting why protons cannot be transported outward. The structure of the four ε-nitrogen atoms from His37 is a good Cu^{2+} chelating site, explaining the inhibition of the channel by Cu^{2+}. Interestingly enough, the opposite orientation of the water molecules near His37 is quite similar to the orientation found in an MD simulation of aquaporin [59]. Such an orientation was suggested to provide an explanation why aquaporin does not conduct protons.

The orientation of His37 in our proposed closed structure does not imply a shuttle mechanism. It was therefore necessary to find an open structure into which the closed structure can evolve upon protonation. This structure was found by a small rotation of the histidine's χ_2 angle from 60° to 0°, which leads to a pore wide enough to let water penetrate through it (Fig. 2b). The close contact between His37 and Trp41 in this open structure favors a cation–π interaction between the two residues. An MD simulation was performed with this open structure in which all histidine residues were in a bi-protonated state in order to examine the previously proposed gating mechanism [39,46]. It was found that the fully bi-protonated state leads to a highly ordered pore water structure whose orientation forbids proton transport from the N-end to the histidine residues.

Combining these results and the previous MS-EVB simulation results, an alternative gating mechanism has been proposed as follows: The closed structure has the (t60, t90, δ) conformation. When the pH_{out} goes down, one (or maybe two) histidine residue becomes bi-protonated, at which point it undergoes a small conformational change by rotating its χ_2 angle from 60° to 0° so that it can be stabilized by its nearest tryptophan residue via a cation–π interaction. This change and other conformational adjustments triggered by it open the pore to let pore water penetrate, forming a proton-conductive water wire through the gate region. Protons can diffuse through channel by hopping through the pore water molecules via the Grotthuss shuttle mechanism. Detailed MD simulations of the entire M2 channel in lipid bilayer will be carried out in the future to help validate and analyze this proposed proton-conductance mechanism.

Acknowledgements: This work was supported by the National Institutes of Health GM53148. Computational support from the Center for High Performance Computing of the University of Utah is gratefully acknowledged.

References

[1] Sugrue, R.J. and Hay, A.J. (1991) Virology 180, 617–624.
[2] Pinto, L.H., Holsinger, L.J. and Lamb, R.A. (1992) Cell 69, 517–528.
[3] Holsinger, L.J., Nichani, D., Pinto, L.H. and Lamb, R.A. (1994) J. Virol. 68, 1551–1563.
[4] Shimbo, K., Brassard, D.L., Lamb, R.A. and Pinto, L.H. (1996) Biophys. J. 70, 1335–1346.
[5] Chizhmakov, I.V., Geraghty, F.M., Ogden, D.C., Hayhurst, A., Antoniou, M. and Hay, A.J. (1996) J. Physiol. 494 (Pt2), 329–336.
[6] Bukrinskaya, A.G., Vorkunova, N.K., Kornilayeva, G.V., Narmanbetova, R.A. and Vorkunova, G.K. (1982) J. Gen. Virol. 60, 49–59.
[7] Martin, K. and Helenius, A. (1991) J. Virol. 65, 232–244.
[8] Sugrue, R.J., Bahadur, G., Zambon, M.C., Hall-Smith, M., Douglas, A.R. and Hay, A.J. (1990) EMBO J. 9, 3469–3476.
[9] Wang, C., Takeuchi, K., Pinto, L.H. and Lamb, R.A. (1993) J. Virol. 67, 5585–5594.
[10] Grambas, S. and Hay, A.J. (1992) Virology 190, 11–18.
[11] Ciampor, F., Thompson, C.A., Grambas, S. and Hay, A.J. (1992) Virus Res. 22, 247–258.
[12] Grambas, S., Bennett, M.S. and Hay, A.J. (1992) Virology 191, 541–549.
[13] Takeuchi, K. and Lamb, R.A. (1994) J. Virol. 68, 911–919.
[14] Lamb, R.A. and Choppin, P.W. (1981) Virology 112, 729–737.
[15] Lamb, R.A., Lai, C.J. and Choppin, P.W. (1981) Proc. Natl. Acad. Sci. USA 78, 4170–4174.
[16] Hull, J.D., Gilmore, R. and Lamb, R.A. (1988) J. Cell Biol. 106, 1489–1498.
[17] Lamb, R.A., Zebedee, S.L. and Richardson, C.D. (1985) Cell 40, 627–633.
[18] Holsinger, L.J. and Lamb, R.A. (1991) Virology 183, 32–43.
[19] Sakaguchi, T., Tu, Q., Pinto, L.H. and Lamb, R.A. (1997) Proc. Natl. Acad. Sci. USA 94, 5000–5005.
[20] Pinto, L.H. et al. (1997) Proc. Natl. Acad. Sci. USA 94, 11301–11306.

[21] Kochendoerfer, G.G., Salom, D., Lear, J.D., Wilk-Orescan, R., Kent, S.B. and DeGrado, W.F. (1999) Biochemistry 38, 11905–11913.
[22] Bauer, C.M., Pinto, L.H., Cross, T.A. and Lamb, R.A. (1999) Virology 254, 196–209.
[23] Salom, D., Hill, B.R., Lear, J.D. and DeGrado, W.F. (2000) Biochemistry 39, 14160–14170.
[24] Tian, C., Tobler, K., Lamb, R.A., Pinto, L.H. and Cross, T.A. (2002) Biochemistry 41, 11294–11300.
[25] Castrucci, M.R., Hughes, M., Calzoletti, L., Donatelli, I., Wells, K., Takada, A. and Kawaoka, Y. (1997) Virology 238, 128–134.
[26] Duff, K.C. and Ashley, R.H. (1992) Virology 190, 485–489.
[27] Duff, K.C., Kelly, S.M., Price, N.C. and Bradshaw, J.P. (1992) FEBS Lett. 311, 256–258.
[28] Kukol, A., Adams, P.D., Rice, L.M., Brunger, A.T. and Arkin, T.I. (1999) J. Mol. Biol. 286, 951–962.
[29] Wang, J., Kim, S., Kovacs, F. and Cross, T.A. (2001) Protein Sci. 10, 2241–2250.
[30] Song, Z., Kovacs, F.A., Wang, J., Denny, J.K., Shekar, S.C., Quine, J.R. and Cross, T.A. (2000) Biophys. J. 79, 767–775.
[31] Kovacs, F.A. and Cross, T.A. (1997) Biophys. J. 73, 2511–2517.
[32] Kovacs, F.A., Denny, J.K., Song, Z., Quine, J.R. and Cross, T.A. (2000) J. Mol. Biol. 295, 117–125.
[33] Kovacs, F.A. and Cross, T.A. (1997) Biophys. J. 73, 2511–2517.
[34] Chizhmakov, I.V., Ogden, D.C., Geraghty, F.M., Hayhurst, A., Skinner, A., Betakova, T. and Hay, A.J. (2003) J. Physiol. 546, 427–438.
[35] Mould, J.A., Drury, J.E., Frings, S.M., Kaupp, U.B., Pekosz, A., Lamb, R.A. and Pinto, L.H. (2000) J. Biol. Chem. 275, 31038–31050.
[36] Wang, C., Lamb, R.A. and Pinto, L.H. (1995) Biophys. J. 69, 1363–1371.
[37] Shuck, K., Lamb, R.A. and Pinto, L.H. (2000) J. Virol. 74, 7755–7761.
[38] Gandhi, C.S., Shuck, K., Lear, J.D., Dieckmann, G.R., DeGrado, W.F., Lamb, R.A. and Pinto, L.H. (1999) J. Biol. Chem. 274, 5474–5482.
[39] Sansom, M.S., Kerr, I.D., Smith, G.R. and Son, H.S. (1997) Virology 233, 163–173.
[40] Zhong, Q., Newns, D.M., Pattnaik, P., Lear, J.D. and Klein, M.L. (2000) FEBS Lett. 473, 195–198.
[41] Zhong, Q., Husslein, T., Moore, P.B., Newns, D.M., Pattnaik, P. and Klein, M.L. (1998) FEBS Lett. 434, 265–271.
[42] Forrest, L.R., Kukol, A., Arkin, I.T., Tieleman, D.P. and Sansom, M.S. (2000) Biophys. J. 78, 55–69.
[43] Forrest, L.R., Tieleman, D.P. and Sansom, M.S. (1999) Biophys. J. 76, 1886–1896.
[44] Smondyrev, A.M. and Voth, G.A. (2002) Biophys. J. 83, 1987–1996.
[45] Schweighofer, K.J. and Pohorille, A. (2000) Biophys. J. 78, 150–163.
[46] Okada, A., Miura, T. and Takeuchi, H. (2001) Biochemistry 40, 6053–6060.
[47] Schmitt, U.W. and Voth, G.A. (2000) Chem. Phys. Lett. 329, 36–41.
[48] Schmitt, U.W. and Voth, G.A. (1998) J. Phys. Chem. B 102, 5547–5551.
[49] Schmitt, U.W. and Voth, G.A. (1999) J. Chem. Phys. 111, 9361–9381.
[50] Schmitt, U.W. and Voth, G.A. (1999) Isr. J. Chem. 39, 483–492.
[51] Cuma, M., Schmitt, U.W. and Voth, G.A. (2000) Chem. Phys. 258, 187–199.
[52] Cuma, M., Schmitt, U.W. and Voth, G.A. (2001) J. Phys. Chem. A 105, 2814–2823.
[53] Day, T.J.F., Soudackov, A.V., Schmitt, U.W. and Voth, G.A. (2002) J. Chem. Phys. 117, 5839–5849.
[54] Tuckerman, M., Laasonen, K., Sprik, M. and Parrinello, M. (1995) J. Chem. Phys. 103, 150–161.
[55] Day, T.J.F., Schmitt, U.W. and Voth, G.A. (2000) J. Am. Chem. Soc. 122, 12027–12028.
[56] Tang, Y., Zaitseva, F., Lamb, R.A. and Pinto, L.H. (2002) J. Biol. Chem. 277, 39880–39886.
[57] Nishimura, K., Kim, S., Zhang, L. and Cross, T.A. (2002) Biochemistry 41, 13170–13177.
[58] Embo JLovell, S.C., Word, J.M., Richardson, J.S. and Richardson, D.C. (2000) Proteins 40, 389–408.
[59] Tajkhorshid, E., Nollert, P., Jensen, M.O., Miercke, L.J., O'Connell, J., Stroud, R.M. and Schulten, K. (2002) Science 296, 525–530.